Verification of filtered Two-Fluid Models in different flow regimes

Jan Hendrik Cloete[1], Schalk Cloete[2], Stefan Radl[3], Shahriar Amini[1,2]*

[1] *Department of Energy and Process Engineering, Norwegian University of Science and Technology (NTNU), NO-7491 Trondheim, Norway*

[2] *Flow Technology Department, SINTEF Materials and Chemistry, NO-7465 Trondheim, Norway*

[3] *Institute of Process and Particle Engineering, Graz University of Technology, Inffeldgasse 13/III, Graz, Austria*

Abstract – This paper compares coarse grid simulations completed with various filtered models to computationally very expensive resolved simulations of fluidization in a 2D setup. It was shown that the original one-marker filtered model performed best. Surprisingly, more recently presented two-marker models showed substantial deviations from the resolved simulations. Unfortunately, one-marker models are not suitable for general large-scale fluidized bed simulations. Therefore, the performance of a new two-marker model is assessed, which respects certain limits when correcting the drag force and uses a normalized filtered slip velocity. While the initial results with this new model are encouraging, substantial uncertainty still exists due to the present lack of a dedicated filtered stress model.

INTRODUCTION

Computational fluid dynamic simulations using the Two-Fluid Model (TFM) closed by the Kinetic Theory of Granular Flow (Gidaspow et al., 1992, Lun et al., 1984) have become a popular tool for the investigation of fluidized beds. This method allows the performance of the reactor to be evaluated and new concepts to be tested without costly experiments or plant trials. However, for accurate results from TFM simulations, it is essential that the transient multiphase structures, i.e. bubbles and clusters, are resolved accurately in time and space (Cloete et al., 2015, 2016b). Despite the rapid increase of computational power over the last few decades, performing resolved simulations remains impractical for large, industrial-scale fluidized beds, especially when small particles (i.e., < 100 µm) are considered.

For this reason filtered TFMs (fTFMs) were developed, with different formulations provided by groups from Princeton (Milioli et al., 2013), INPT (Ozel et al., 2013) and JKU (Schneiderbauer and Pirker, 2014). In this approach, the conservation equations are spatially averaged, with additional terms appearing for the effects of the unresolved, meso-scale structures on the drag force and the solids stresses. Data from highly resolved simulations are then analyzed by statistically averaging over differently sized regions (filters) to develop correlations for these additional terms. Consequently, reasonable predictions of overall reactor behavior can be obtained in coarse grid simulations at computational times that are several orders of magnitude smaller than what would be required for resolved simulations. Most of the research in the field has focused on developing a filtered drag model, since the contribution of the drag term is generally most important in the filtered momentum equations (Ozel et al., 2013).

The current state-of-the-art filtered drag models are two-marker models. Here the corrections for sub-grid effects are described (next to the averaging volume, i.e., filter size) as a function of (i) the filtered solids volume fraction, and (ii) the filtered solids slip velocity. The filtered slip velocity will tend to increase in less homogenous flows as the gas will tend to bypass dense regions, creating a larger slip between the phases inside the filter region. The filtered slip velocity therefore acts as a measure of the non-homogeneity of the flow and therefore serves as a good choice as independent variable in correlations for the sub-grid corrections. One disadvantage of the slip velocity, however, is that it is highly correlated with the volume fraction. For example, larger slip velocities will tend to occur in dilute regions, whereas the slip velocities will tend to be smaller in dense regions. This leads to a situation where the occurrences are distributed unevenly in the two-dimensional parameter space, making it more difficult to fit an accurate model to the data.

Our present contribution proposes the filtered slip velocity magnitude scaled by the steady state slip velocity as a second marker for the drag correction correlation. Since the steady state slip velocity is a function of the filtered solids volume fraction, it results in a much more even distribution of data in the two-dimensional parameter space. Additionally, a simple dependency of the drag correction on the scaled filtered slip velocity was revealed, which allows a correlation to be accurately fitted to the data. The resulting model is tested in this study by comparing coarse grid simulation results with resolved simulation results, as well as to coarse

grid simulations from filtered drag models previously proposed in literature, for 3 cases operating in different fluidization regimes. This will show the potential of this approach for future study.

SIMULATIONS

Resolved simulations

Fine grid simulations are performed in this study for the evaluation of the filtered models in coarse grid simulations using the Two Fluid Model closed by the Kinetic Theory of Granular Flow. A more detailed description of the resolved simulation setup can be found in (Cloete et al.).

Filtered simulations

The coarse grid simulations are performed using the spatially averaged, or filtered, continuity and momentum equations. The filtered continuity equations remain similar in form to the equations used in the resolved simulations. However, the filtered momentum equations contain several additional terms that require closure, as shown for the filtered solids momentum equation below. The filtered gas momentum equation contains similar terms, but the gas phase meso-scale stresses are generally considered to be small (Milioli et al., 2013) and are therefore neglected in this study.

$$\frac{\partial}{\partial t}\left(\rho_s \overline{\alpha_s}\widetilde{\vec{\upsilon}_s}\right)+\nabla\cdot\left(\rho_s \overline{\alpha_s}\widetilde{\vec{\upsilon}_s}\widetilde{\vec{\upsilon}_s}\right)=-\overline{\alpha_s}\nabla\overline{p}-\nabla\overline{p_s}-\nabla\cdot\left(\rho_s\overline{\alpha_s\vec{\upsilon}_s'\vec{\upsilon}_s'}\right)+ \nabla\cdot\overline{\overline{\tau}}_s+\overline{\alpha_s}\rho_s\vec{g}+\overline{K_{gs}\left(\vec{\upsilon}_g-\vec{\upsilon}_s\right)}-\overline{\alpha_s'\nabla p'} \tag{1}$$

Here, the third term on the right requires closure for the meso-scale solids stresses, and the two last terms require closure for the meso-scale interphase momentum exchange. Three literature formulations of these closures will be evaluated (Igci and Sundaresan, 2011, Milioli et al., 2013, Sarkar et al., 2016) in what follows. In addition, this study will evaluate a new filtered drag model.

The closure for the filtered drag force is usually determined in the following form:

$$C=\frac{\overline{K_{gs}\left(\upsilon_{g,y}-\upsilon_{s,y}\right)-\alpha_s'\dfrac{dp'}{dy}}}{K_{gs,coarse}\left(\tilde{\upsilon}_{g,y}-\tilde{\upsilon}_{s,y}\right)} \tag{2}$$

where $K_{gs,coarse}$ is evaluated at the filtered solids volume fraction and filtered slip velocity. Note, that only the forces and slip velocities in the *y*-direction are considered when calculating C (i.e., the drag correction factor) since the filtered drag force is most important in that direction.

The following equation is proposed for the filtered drag correction factor:

$$-\log\left(C\right)=\frac{\arctan\left(x_1\left(\Delta_f^*-\Delta_{fine}^*\right)^{x_7}\overline{\alpha}_s\right)\arctan\left(x_2\left(\Delta_f^*-\Delta_{fine}^*\right)^{x_8}\left(\overline{\alpha}_{\max}-\overline{\alpha}_s\right)\right)}{\arctan\left(x_3\left(\Delta_f^*-\Delta_{fine}^*\right)\right)\left(x_4\log\tilde{\upsilon}_{slip}^*-x_5\left(\Delta_f^*-\Delta_{fine}^*\right)^{x_6}\right)}\Bigg/\left(\frac{\pi}{2}\right)^3 \tag{3}$$

where $\tilde{\upsilon}_{slip}^*$ (the scaled filtered slip velocity magnitude) is the filtered slip velocity magnitude divided by the steady state slip velocity at the filtered solids volume fraction and Δ_{fine}^* is the dimensionless grid size in the resolved simulations used to develop the model. The filter size is non-dimensionalized by $\Delta_f^*=\Delta_f g/v_t^2$. The following values of the coefficients are used: $x_1=32.3$, $x_2=53.7$, $x_3=16.0$, $x_4=0.933$, $x_5=0.0327$, $x_6=0.746$, $x_7=0.870$, $x_8=0.962$, and $\bar{\alpha}_{max}=0.55$. The fine grid scaled filter size is set to $\Delta_{fine}^*=0.129$.

This approach offers several improvements over the current state-of-the-art two-marker models (Milioli et al., 2013, Sarkar et al., 2016). Firstly, using the scaled filtered slip velocity as the second marker leads to a more even distribution of data in the two-dimensional parameter space when collecting data from resolved simulations. This allows a more accurate model to be fitted to the data. Secondly, by fitting a correlation to $-\log\left(C\right)$, more emphasis is placed on large corrections, therefore improving the model fit in regions where the filtered drag correction is most important. Thirdly, we find that using the scaled filtered slip velocity results in a linear dependency of $-\log\left(C\right)$ on $\log\tilde{\upsilon}_{slip}^*$. This allows a simpler correlation to be chosen as the basis of our fit.

Lastly, the equation form proposed obeys all the physical constraints for the filtered drag correction: the first and the second arctan functions cause a zero correction for very dilute and very dense flows, when there are no meso-scale structures. The third arctan function leads to a zero correction when the filter size is equal to the grid size used in the resolved simulations, and causes the drag correction to reach an asymptotic limit at very large filter sizes. Last, the correction C is ensured to be positive due to the nature of logarithmic functions.

Verification cases

Three cases, operated in different fluidization regimes, are considered to thoroughly test the generality of the filtered models derived in this study. The average superficial inlet gas velocity is chosen to be at the geometric center of the bubbling fluidization and turbulent fluidization regimes, according to (Bi and Grace, 1995), and quarter way between the transitions to turbulent fluidization and homogenous dilute phase transport for the fast fluidization case. A solids flux of 150 kg/m^2s is specified, and the simulation was run for 10s to reach a pseudo-steady state before time-averaging the simulation for 30s.

Additionally, the profile of the velocity and solids volume fraction at the inlet is specified to be non-uniform. This forces a mean gradient in the system, allowing for rigorous testing of the filtered models for the meso-scale solids stresses. The gas phase superficial velocity is chosen to be half the average superficial velocity at the sides of the domain and increase linearly towards the center. The solids inlet velocity is set equal to the gas inlet velocity. The solid volume fraction is set to a minimum at the centre, with a value equal to half the solids volume fraction required to deliver the specified solids flux at the mean gas superficial velocity. The solids volume fraction then increases linearly towards the sides.

The average superficial velocity for each case is given in Table 1, as well as the geometrical proportions. Figure 2 to Figure 4 offer graphical examples of the three simulated geometries. The simulation domain consists of a rectangular reactor region and a small outlet region. The aspect ratio of the reactor region is increased with a factor of 2 as the fluidization velocity is increased to allow sufficient cluster formation inside the fluidization region. The sides of the fluidization region are specified as periodic boundaries, since the model evaluated in this study was derived for periodic flows not influenced by wall-effects. In the outlet region, walls with a free-slip boundary condition for the solids slope at an angle of 45° towards the outlet. The outlet has a width of 10 cm to prevent backflow, which would cause numerical instabilities. The average solids volume fraction in the rest of the study is evaluated in the fluidization region only, to minimize the influence of the walls in the outlet region on the results.

Table 1 - Description of the configuration for the three verification cases

Case	Fluidization region height (m)	Fluidization region width (m)	Average gas superficial velocity (m/s)
Bubbling	1.6	0.96	0.468
Turbulent	2.26	0.679	2.07
Fast fluidization	3.2	0.48	5.01

All simulations were performed in 2D to allow feasible computational times of the resolved simulations, which were performed at a grid size equal to 11.8 times the particle diameter. Testing filtered models in 2D should, however, still remain a valid approach, since filtered models derived from 2D and 3D simulations have been shown to be qualitatively similar (Igci et al., 2008). The particle and fluid properties used in the simulations are summarized in Table 2.

Table 2 - Summary of particle and fluid properties

d	Particle diameter	75×10^{-6} m
ρ_s	Particle density	1500 kg/m^3
ρ_g	Gas density	1.3 kg/m^3
μ_g	Gas viscosity	1.8×10^{-5} kg/m s
v_t	Terminal settling velocity	0.2184 m/s

RESULTS AND DISCUSSION

Model performance comparison

An overall view of model performance is shown in Figure 1. The bars represent the percentage deviation in terms of overall solids hold-up from the fine-grid simulations for the three different fluidization regimes. A positive deviation implies that too much solids is present in the domain, most likely caused by an under-prediction of the drag force. A negative deviation indicates too little solids resulting from an over-predicted drag force.

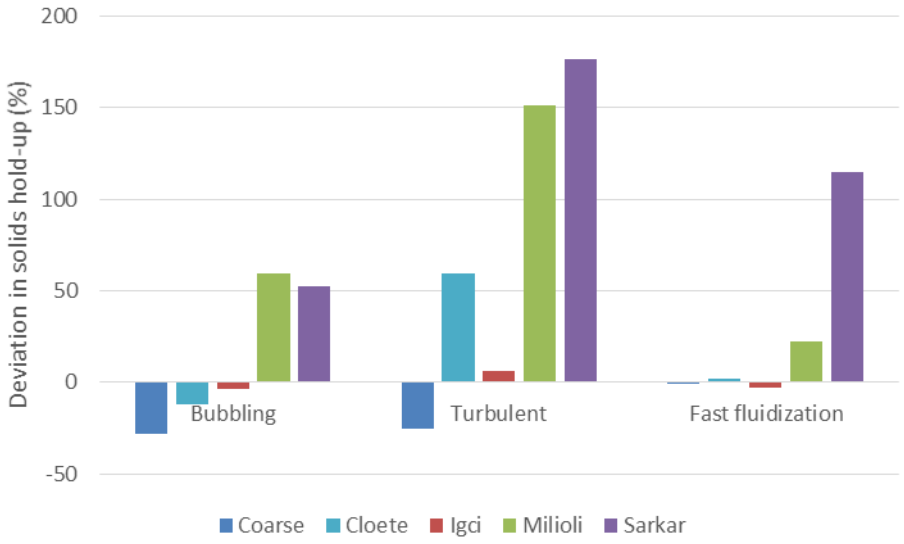

Figure 1: Deviation in the overall solids holdup from the resolved simulation for several different model setups. Coarse: no filtered modelling; Cloete: Equation (3); Igci: (Igci and Sundaresan, 2011); Milioli: (Milioli et al., 2013); Sarkar: (Sarkar et al., 2016). All simulations were carried out on a grid size of 20 mm (~23 times larger than the fine grid simulations).

The importance of a filtered model is clearly visible in the Coarse simulations for the bubbling and turbulent regimes shown in Figure 1. In both these cases, a significant negative deviation (i.e., ca. 25%) in the overall solids hold-up is observed, indicating that clustering is not sufficiently resolved to accurately predict the momentum coupling between gas and solids. As a result, the momentum coupling term is over-predicted, resulting in an under-prediction of the solids hold-up. This is not observed in the fast fluidization regime case because clustering only took place in a relatively small region of the domain (see Figure 4).

Of the four different filtered models employed, the Igci model consistently showed the best performance. This is the original filtered model, using only the filtered volume fraction as a marker for both the drag and the stresses. Also, the Igci model has been derived from 2D simulations. Unfortunately, this model is not suitable as a general solution for large-scale fluidized bed reactor modelling because of two important limitations: (i) it requires specialized wall functions to give reliable predictions in wall-bound domains (Cloete et al., 2013), and (ii) it cannot create sufficiently large drag corrections to predict flows in domains with very large cell sizes (Cloete et al., 2016a).

The more complex two-marker models, which employ the filtered slip velocity as an additional marker for the drag and the filtered scalar strain rate as an additional marker for the stresses, proved to be less reliable. These models are required to overcome the fundamental limitations of the one-marker model outlined above, but it is clear that additional work is required to improve performance to the point where these models can be safely employed for large-scale fluidized bed reactor simulations.

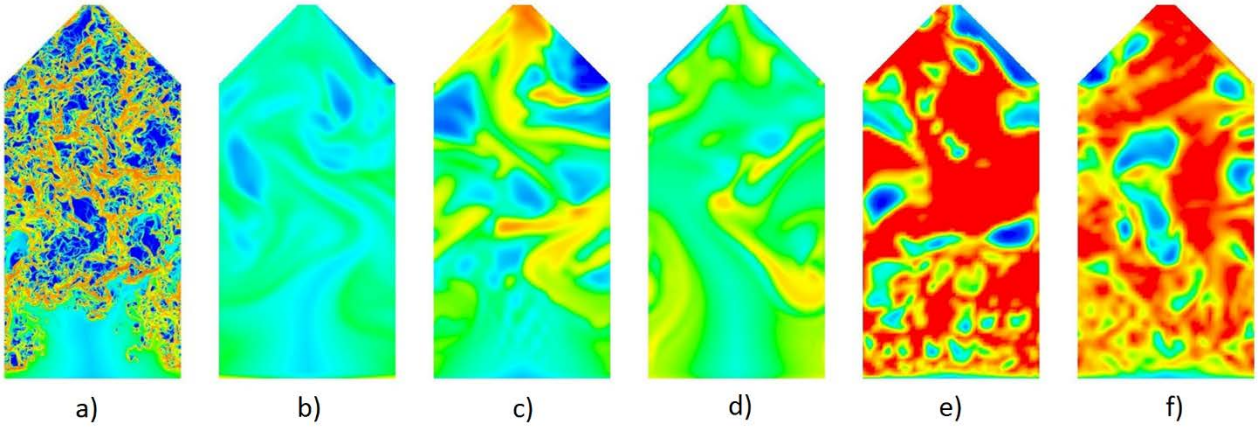

Figure 2: Instantaneous solids volume fraction contours arranged from left to right for the (a) Resolved, (b) Coarse, (c) Cloete, (d) Igci, (e) Milioli and (f) Sarkar models in the bubbling regime. The models are referenced in the caption of Figure 1.

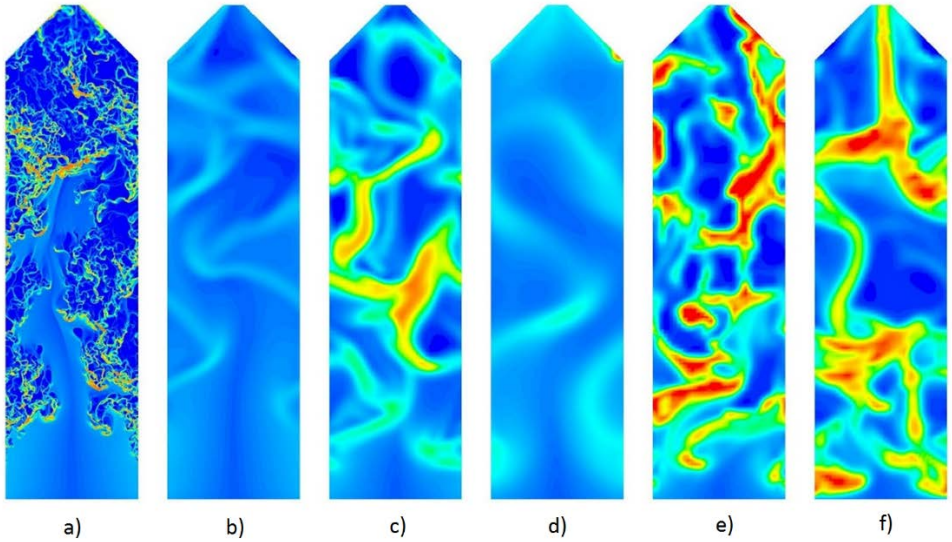

Figure 3: Instantaneous solids volume fraction contours arranged from left to right for the (a) Resolved, (b) Coarse, (c) Cloete, (d) Igci, (e) Milioli and (f) Sarkar models in the turbulent regime. The models are referenced in the caption of Figure 1.

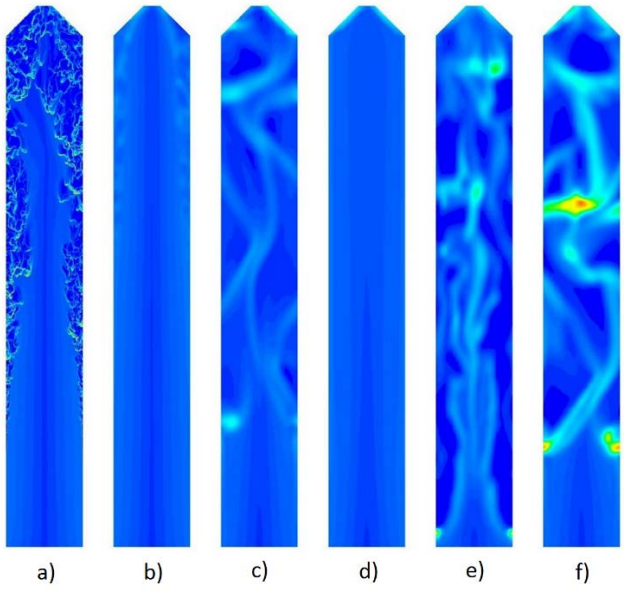

Figure 4: Instantaneous solids volume fraction contours arranged from left to right for the (a) Resolved, (b) Coarse, (c) Cloete, (d) Igci, (e) Milioli and (f) Sarkar models in the fast fluidization regime. The models are referenced in the caption of Figure 1.

As shown in Figure 2, Figure 3 and Figure 4, both the Milioli and Sarkar models lead to large inaccuracies when compared to the resolved simulation. Not only is the solids hold-up much too high, but the bottom region where no clustering takes place is not captured correctly. Given that the Sarkar model was derived for 3D flows, it is understandable that the drag force is under-predicted. However, such a clear reason for the discrepancy cannot be identified for the Milioli model. The Cloete model performs better, both in terms of overall solids hold-up and qualitative flow behavior, but significant discrepancies are still evident.

It is important to note that the Cloete filtered drag model was implemented with the Sarkar filtered stresses, which gave the most accurate results in all three cases. Figure 5 shows that the filtered stress model has a significant impact on the solids hold-up and the general flow behavior in the filtered simulation. It is therefore recommended that care should be taken when deriving filtered models for solids pressure and viscosity since these models strongly impact the accuracy of the overall filtered simulation.

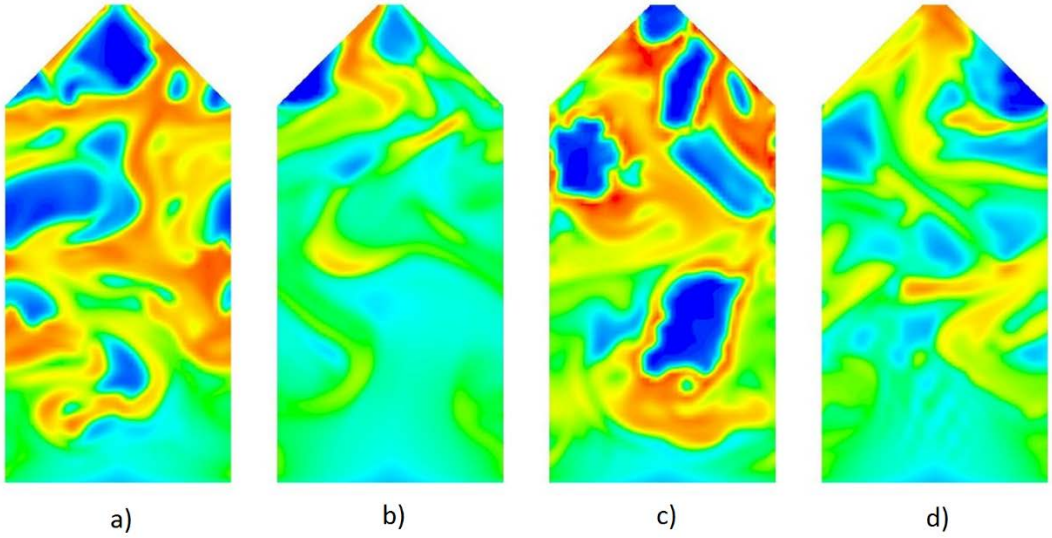

Figure 5: Instantaneous solids volume fraction contours for the Cloete filtered drag model with (a) no filtered stress modelling, (b) Igci filtered stresses, (c) Milioli filtered stresses and (d) Sarkar filtered stresses in the bubbling regime. The models are referenced in the caption of Figure 1.

Drag model comparison

In order to better understand the results presented thus far, the drag correction functions of the four different filtered drag models investigated in this study are represented in Figure 6. Most important, the wide range of drag corrections accessible by the two-marker models relative to the one marker model is clearly visible. In addition, the large filtered drag corrections predicted by the Milioli and Sarkar models relative to the Cloete and Igci models are also evident. This helps to explain the trends shown in Figure 1.

The four filtered drag models share similar characteristics. All the two-marker models increase the drag correction with an increase in the slip velocity. In addition, all the models except for Sarkar respect the physical limits that no drag correction is present at zero and very high filtered solids volume fractions (no clusters can form under these conditions). The large drag correction predicted by the Sarkar model at high solids volume fractions and scaled slip velocities could lead to unphysical results.

It is also noteworthy that the Milioli and Sarkar models encounter a maximum bound within the range of scaled slip velocities investigated. Such a maximum bound could restrict the generality of the model, especially when large cell sizes are used in large-scale filtered fluidized bed simulations. Another important fundamental challenge with the Milioli and Sarkar formulations is that the drag correction sometimes increases with the slip velocity to a power greater than unity. This characteristic causes the drag force in a filtered simulation to decrease with increased slip velocity, creating an unphysical self-reinforcing feedback mechanism where more slip leads to less drag and even more slip.

The Cloete model attempts to rectify these issues by respecting all physical limits (including the fact that the drag force must increase with slip velocity) and not imposing a maximum correction. As stated in the methodology, this correlation also ensures a relatively even distribution of data throughout the parameter space, thereby maximizing the likelihood of a good correlation fit. It therefore appears to be a good foundation on which to build an improved set of two-marker filtered models.

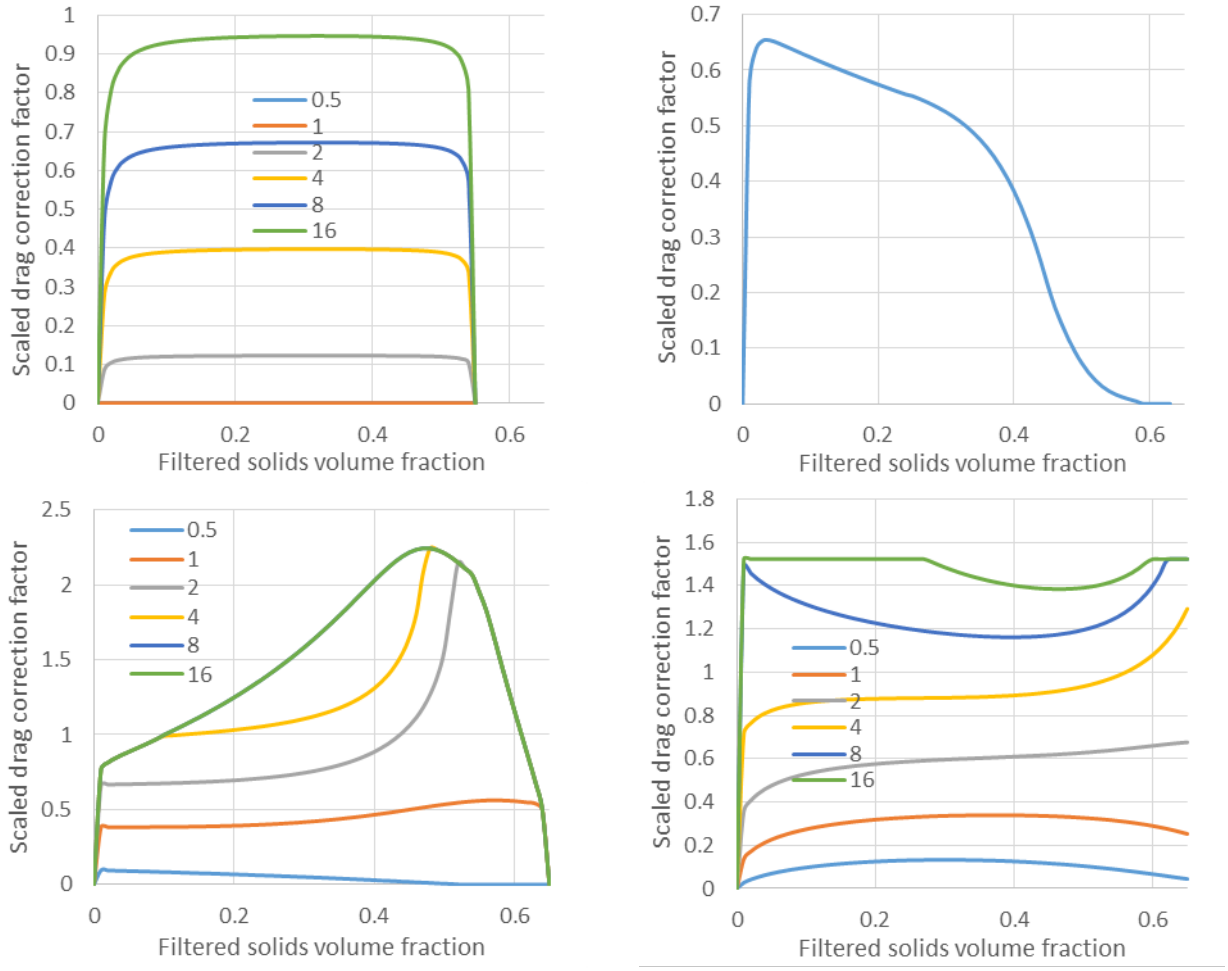

Figure 6: Graphical representation of the drag corrections of Cloete (top left), Igci (top right), Milioli (bottom left) and Sarkar (bottom right) expressed as $-log(C)$. The different lines represent different scaled slip velocities ranging from 0.5 to 16. The models are referenced in the caption of Figure 1.

CONCLUSIONS

This verification study has illustrated that substantial research efforts are still required to develop filtered models that are suitable for general application in large-scale fluidized bed reactor simulations. Verification studies in 2D domains and over three fluidization regimes; bubbling, turbulent and fast fluidization, have illustrated that the simple original one-marker filtered model results in accurate predictions, whereas more recent two-marker models show substantial deviations from well-resolved verification simulations.

Given that the one-marker approach is not suitable as a general large scale fluidized bed modelling solution, two-marker model development studies should continue. One such new two-marker drag model was tested with improved results relative to existing models. However, evaluation of the new model involved significant uncertainty because a dedicated solids stress model is not yet available. It was shown that the implementation of different available solids stress models with the new drag model resulted in widely different solutions.

The new proposed two-marker drag correlation aims to improve on existing models by evenly distributing the data in bins within the 2D parameter space, respecting physical limits, avoiding a maximum bound on the correction and devising a simple equation form that is easy to implement. Despite the uncertainty introduced by the solids stress model, the results presented in this paper are encouraging. Future work will derive dedicated models for solids pressure and viscosity in order to more conclusively verify the performance of this new drag correlation.

NOTATION

ρ	density, kg/m^3	C	Filtered drag correction factor
α	volume fraction	Δ_f^*	Dimensionless filter size
p	pressure, Pa	d	Particle diameter, m
υ	velocity, m/s	$\tilde{\upsilon}_{slip}^*$	Scaled filtered slip velocity magnitude, m/s
g	gravitational constant, m/s^2	μ_g	Gas viscosity, kg/m s
K_{gs}	Momentum exchange coefficient		

ACKNOWLEDGEMENT

The authors would like to express their gratitude for the financial support from the European Commission under the NanoSim grant (project number: 604656), as well as for the computational resources provided at NTNU by UNINETT Sigma2 AS, https://www.sigma2.no.

REFERENCES

Bi, H. T., and J. R. Grace. 1995. Flow regime diagrams for gas-solid fluidization and upward transport. *International Journal of Multiphase Flow* 21 (6):1229-1236.

Cloete, Jan Hendrik, Schalk Cloete, Federico Municchi, Stefan Radl, and Shahriar Amini. The sensitivity of filtered Two Fluid Model to the underlying resolved simulation setup. *Powder Technology*.

Cloete, S., J. H. Cloete, and S. Amini. 2016a. "Comparison of the Filtered Two Fluid Model and Dense Discrete Phase Model for Large-Scale Fluidized Bed Reactor Simulations." AIChE Annual Meeting, San Franciso, USA.

Cloete, Schalk, Stein Tore Johansen, and Shahriar Amini. 2013. Evaluation of a filtered model for the simulation of large scale bubbling and turbulent fluidized beds. *Powder Technology* 235 (0):91-102.

Cloete, Schalk, Stein Tore Johansen, and Shahriar Amini. 2015. Grid independence behaviour of fluidized bed reactor simulations using the Two Fluid Model: Effect of particle size. *Powder Technology* 269:153-165.

Cloete, Schalk, Stein Tore Johansen, and Shahriar Amini. 2016b. Grid independence behaviour of fluidized bed reactor simulations using the Two Fluid Model: Detailed parametric study. *Powder Technology* 289:65-70.

Gidaspow, D. , R. Bezburuah, and J. Ding. 1992. "Hydrodynamics of Circulating Fluidized Beds, Kinetic Theory Approach." 7th Engineering Foundation Conference on Fluidization

Igci, Y., A. T. Andrews, S. Sundaresan, S. Pannala, and T. O'Brien. 2008. Filtered two-fluid models for fluidized gas-particle suspensions. *AIChE Journal* 54 (6):1431-1448.

Igci, Yesim, and Sankaran Sundaresan. 2011. Constitutive Models for Filtered Two-Fluid Models of Fluidized Gas–Particle Flows. *Industrial & Engineering Chemistry Research* 50 (23):13190-13201.

Lun, C.K.K, S.B. Savage, D.J. Jeffrey, and N. Chepurniy. 1984. Kinetic Theories for Granular Flow: Inelastic Particles in Couette Flow and Slightly Inelastic Particles in a General Flow Field. *Journal of Fluid Mechanics* 140:223-256.

Milioli, Christian C., Fernando E. Milioli, William Holloway, Kapil Agrawal, and Sankaran Sundaresan. 2013. Filtered two-fluid models of fluidized gas-particle flows: New constitutive relations. *AIChE Journal* 59 (9):3265-3275.

Ozel, A., P. Fede, and O. Simonin. 2013. Development of filtered Euler–Euler two-phase model for circulating fluidised bed: High resolution simulation, formulation and a priori analyses. *International Journal of Multiphase Flow* 55 (0):43-63.

Sarkar, Avik, Fernando E. Milioli, Shailesh Ozarkar, Tingwen Li, Xin Sun, and Sankaran Sundaresan. 2016. Filtered sub-grid constitutive models for fluidized gas-particle flows constructed from 3-D simulations. *Chemical Engineering Science* 152:443-456.

Schneiderbauer, Simon, and Stefan Pirker. 2014. Filtered and heterogeneity-based subgrid modifications for gas–solid drag and solid stresses in bubbling fluidized beds. *AIChE Journal* 60 (3):839-854.